

APPLIED COMPUTING, MATHEMATICS AND STATISTICS GROUP

Division of Applied Management and Computing

Scale Dependent Solute Dispersion in Porous Media

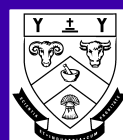
Channa Rajanayaka and Don Kulasiri

Research Report 01/2003
January 2003

ISSN 1174-6696

RESEARCH REPORT

LINCOLN
UNIVERSITY
Te Whare Wānaka O Aoraki



Applied Computing, Mathematics and Statistics

The Applied Computing, Mathematics and Statistics Group (ACMS) comprises staff of the Applied Management and Computing Division at Lincoln University whose research and teaching interests are in computing and quantitative disciplines. Previously this group was the academic section of the Centre for Computing and Biometrics at Lincoln University.

The group teaches subjects leading to a Bachelor of Applied Computing degree and a computing major in the Bachelor of Commerce and Management. In addition, it contributes computing, statistics and mathematics subjects to a wide range of other Lincoln University degrees. In particular students can take a computing and mathematics major in the BSc.

The ACMS group is strongly involved in postgraduate teaching leading to honours, masters and PhD degrees. Research interests are in modelling and simulation, applied statistics, end user computing, computer assisted learning, aspects of computer networking, geometric modelling and visualisation.

Research Reports

Every paper appearing in this series has undergone editorial review within the ACMS group. The editorial panel is selected by an editor who is appointed by the Chair of the Applied Management and Computing Division Research Committee.

The views expressed in this paper are not necessarily the same as those held by members of the editorial panel. The accuracy of the information presented in this paper is the sole responsibility of the authors.

This series is a continuation of the series "Centre for Computing and Biometrics Research Report" ISSN 1173-8405.

Copyright

Copyright remains with the authors. Unless otherwise stated permission to copy for research or teaching purposes is granted on the condition that the authors and the series are given due acknowledgement. Reproduction in any form for purposes other than research or teaching is forbidden unless prior written permission has been obtained from the authors.

Correspondence

This paper represents work to date and may not necessarily form the basis for the authors' final conclusions relating to this topic. It is likely, however, that the paper will appear in some form in a journal or in conference proceedings in the near future. The authors would be pleased to receive correspondence in connection with any of the issues raised in this paper. Please contact the authors either by email or by writing to the address below.

Any correspondence concerning the series should be sent to:

The Editor
Applied Computing, Mathematics and Statistics Group
Applied Management and Computing Division
PO Box 84
Lincoln University
Canterbury
NEW ZEALAND

Email: computing@lincoln.ac.nz

SCALE DEPENDENT SOLUTE DISPERSION IN POROUS MEDIA

Channa Rajanayaka and Don Kulasiri

*Centre for Advanced Computational Solutions (C-fACS), Applied Computing, Mathematics and Statistics Group
Lincoln University, PO Box 84, Canterbury, New Zealand (rajanayc@lincoln.ac.nz)*

Abstract Scale dependency of solute dispersion in porous media is one of the major striking issues in simulating larger scale aquifers. There are numerous studies dedicated to development of the simulation models that represent heterogeneous real world aquifers. In this paper we investigated the ability of a stochastic solute transport model (SSTM) of capturing the scale dependency. Initially, flow profiles were visually compared for different flow lengths. Then a stochastic inverse method was used to estimate the corresponding dispersion coefficient (D) for each parameter combination of the stochastic model. The results reveal that SSTM is capable of simulating the scale effect of solute dispersion, and to some extent, they agree with the past literature. Dispersivity increases with the smaller flow lengths, and the rate of increase decreases and tends to reach an asymptotic value for larger scales for similar parameters of SSTM.

Keywords: Scale Dependency; Simulation; Stochastic Modeling; Groundwater; Solute Transport

1. INTRODUCTION

We model the behavior of natural systems using basic laws of physics that govern the system by means of a mathematical representation. The advection-dispersion equation is widely used to simulate the solute transport through porous media using parameters such as hydraulic conductivity, porosity, and dispersivity [Fetter, 1999]. In deriving this equation, based on macroscopic mass balance, we average the volumetric flux of the solute transported by the average flow. The total solute flux at a given point is the sum of the mean flux and the fluctuating component, which occurs as a result of noise introduced into the flow by irregular porous media. This mean transport of the solute is called the advective flux, and the fluctuating component of the flux above the mean is given as the dispersive flux. Such fluctuations do not exist in zero mean flow velocity and progressively increase with the flow. Further, if the concentration of solute were different at two locations, it would affect the net transport of the solute mass. Hence, based on plausible arguments, the dispersive flux can be assumed to be proportional to the mean velocity and the concentration gradient [for a detailed discussion refer to

Kulasiri and Verwoerd, 2002]. This argument is reminiscent of Fick's law and the dispersion (molecular diffusion plus mechanical dispersion) is approximated by the dispersion coefficient, $D = \alpha_L v$, where α_L is the longitudinal dispersivity, and v is the mean velocity. However, it is well known that D is scale dependent [Fetter, 1999].

1.1 Scale Dependency

Theis [1962, 1963] argued that the increased longitudinal dispersion observed in the field experiments, compared to the laboratory experiments, may be resulting from the wide distribution of permeabilities and consequently velocities found within an aquifer. Fried [1972] presented a few longitudinal dispersivity observations for several sites, which were 0.1 to 0.6 m for the local (aquifer stratum) scale, 5 to 11 m for the global (aquifer thickness) scale. Fried [1975] revisited and redefined these scales in terms of 'mean traveled distance' of the tracer or contaminant as (i) local scale, between 2 and 4 m, (ii) global scale 1, between 4 and 20 m, (iii) global scale 2, between 20 and 100 m, and (iv) regional scale, larger than 100 m (usually several kilometers).

Fried [1972] found no scale effect on the transverse dispersion coefficient and suggested that its value could be obtained from laboratory results. However, Klotz et al. [1980] illustrated from a field tracer test that the width of the tracer plume increased linearly with travel distance. Oakes and Edworthy [1977] conducted two-well pulse and radial injection experiments in a sandstone aquifer and showed that the dispersivity readings for the fully penetrated depth to be 2 to 4 times the values for discrete layers.

Pickens and Grisak [1981] conducted laboratory column and field tracer tests to investigate the magnitude of longitudinal dispersivity, α_L , in a sandy stratified aquifer. The average α_L of 0.035 cm was obtained for three laboratory tracer tests with a repacked column of sand when the flow length was 30 cm. The analysis of the withdrawal phase concentration history for the injection withdrawal well of a single-well test showed an α_L of 3 cm and 9 cm for flow lengths of 3.13 m and 4.99 m, respectively. Further, they

obtained 50 cm dispersivity in a two-well recirculating withdrawal-injection tracer test with wells located 8 m apart. All the above mentioned tests were conducted in the same site. Pickens and Grisak [1981] showed that the scale dependency of α_L for the study site has a relationship of $\alpha_L = 0.1 L$, where L is the mean travel distance. Lallemand-Barres and Peaudecerf [1978] plotted the field measured α_L against the flow length on a log-log paper. This graph strengthens the finding of Pickens and Grisak [1981]. Gelhar [1986] published a similar representation of the scale dependency of α_L . That study was conducted with the data from many sites around the world, and indicated that α_L in the range of 1 to 10 m would be reasonable for a site of dimension in the order of 1 km. However, the plot suggests that relationship between α_L and the flow length is more complex and not as straightforward as shown by Pickens and Grisak [1981], and Lallemand-Barres and Peaudecerf [1978]. Huang et al. [1996a] developed an analytical solution for solute transport in heterogeneous porous media with scale dependent dispersion. In this model, dispersivity increases linearly with the flow length until some distance and reaches an asymptotic process. Other studies on scale dependency of dispersivity can be found in Huang et al. [1996b], Scheibe and Yabusaki [1998], Klenk and Grathwohl [2002], and Vanderborgh and Vereecken [2002].

The above studies clearly manifest that dispersivity of solute transport in porous media is not only scale dependent but also a complex phenomenon. Nevertheless, groundwater contamination issues are so predominant and necessity of dealing with larger scale aquifers is unavoidable. The complex occurrence like scale dependency of dispersivity shows that some natural phenomena cannot be explained by using the models that give deterministic solutions, which have a single set of output values for a given set of inputs and parameters. Furthermore, the formation of real world natural systems like groundwater aquifers are highly heterogeneous, boundaries of the system are multifaceted, inputs are highly erratic and other subsidiary conditions can be subject to variation as well. Non-homogeneous formation of natural porous mediums was illustrated by Øksendal [1998]. They injected color liquid into a body of porous rock material and showed that the resulting scattered distribution of the liquid was not diffusing according to the deterministic model. The permeability of the porous medium varied within the material in an irregular manner. Therefore, uncertainty has to be incorporated in the model. For this reason, the stochastic models are more representative of heterogeneous systems and can incorporate this uncertainty by using stochastic differential equations.

The objective of this paper is to investigate a stochastic solute transport model (SSTM) [Kulasiri and Verwoerd, 1999, 2002] to assess its ability to capture the scale dependency of D . The main feature of this model is it assumes the velocity of solute as a fundamental stochastic variable, $v(x,t) = \bar{v}(x,t) + \xi(x,t)$, where $\bar{v}(x,t)$ = average velocity described by Darcy's law and $\xi(x,t)$ = white noise correlated in space and δ -correlated in time. This model avoids the use of the Fickian assumptions that give rise to the dispersion coefficient, D . As a result, the scale dependent D would not affect the model solution. Therefore, it is important to investigate whether the model could capture the scale effect in representing stochastic flow.

2. STOCHASTIC MODEL

A detail description the stochastic model can be found in Kulasiri and Verwoerd [1999, 2002], and a brief introduction is given here that enables the reader to easily refer to the essential components of the model. The formulation of SSTM can be expressed by the following stochastic partial differential equation;

$$dC = S(\bar{v}(x,t)C(x,t))dt + S(C(x,t)d\beta(t)), \quad (1)$$

where \bar{v} = mean velocity,

$$d\beta_m(t) = \sum_{j=1}^m f_j \sqrt{\lambda_j} db_j(t), \quad (2)$$

m = number of terms used,

$db_j(t)$ = increments of standard Wiener processes,

f_j = eigenfunctions of velocity covariance function,

λ_j = eigenvalues of velocity covariance function,

$S = -\left(\frac{h_x}{2} \frac{\partial^2}{\partial x^2} + \frac{\partial}{\partial x}\right)$ is an operator in space, and

$h_x = dx$.

An exponential covariance kernel was assumed based on plausible arguments to model the spatial correlation of the noise component of the velocity function, and that can be given by

$$q(x_1, x_2) = \sigma^2 e^{-\frac{|y|}{b}}, \quad (3)$$

where $y = |x_1 - x_2|$,

b = correlation length, and

σ^2 = variance.

x_1 and x_2 are any two points within the spatial range, $[0, a]$, considered. The eigenfunctions, f_n and eigenvalues,

λ_n of $q(x_1, x_2)$ are obtained as the solution to the following integral equation:

$$\int_0^a q(x_1, x_2) f_n(x_2) dx_2 = \lambda_n f_n(x_1). \quad (4)$$

Assuming σ^2 is a constant over $[0, a]$, the solution to (4) can be obtained by:

$$\lambda_n = \frac{2\theta\sigma^2}{\omega_n^2 - \theta^2}, \quad (5)$$

where $\theta = 1/b$ and ω_n s are the roots of the following equation:

$$\tan \omega_n a = \frac{2\omega_n \theta}{\omega_n^2 - \theta^2}. \quad (6)$$

The basic function of (2) can be obtained by solving (4). The n^{th} basis function is given by

$$f_n(x) = \frac{1}{\sqrt{N}} \left(\sin \omega_n x + \frac{\omega_n}{\theta} \cos \omega_n x \right), \quad (7)$$

$$\text{where } N = \frac{1}{2} a \left(1 + \frac{\omega^2}{\theta^2} \right) - \frac{1}{4\omega} \left(1 + \frac{\omega^2}{\theta^2} \right) \sin 2\omega a - \frac{1}{2\theta} (\cos 2\omega a - 1). \quad (8)$$

3. COMPUTATIONAL INVESTIGATION

The main parameters of the model are the correlation length, b and the variance, σ^2 . The statistical nature of the computational solution changes with different b and σ^2 . Distributed concentration values of (1) were obtained by using the finite difference numerical solution taking the numerical convergence and stability into account [Kulasiri and Verwoerd, 2002]. We solved (6) to generate the roots for a given set of parameters. Generally 29 terms are more than sufficient to produce converging numerical solution. We generated the standard Wiener process increments in Hilbert space for the time intervals of 0.001 days. Then eigenvalues λ_n of (5) were computed for the required σ^2 . With these roots, ω and λ_n , we calculated the basic function (7). Those values were used to generate $d\beta(t)$ in (2). The numerical scheme of SSTM was then used to calculate the concentration profile for spatial-temporal development for the mean velocity of 0.5 m/day.

We used spatial grid length of 0.1 m for the numerical calculation. Initial concentration value of 1.0 unit was considered at $x = 0$ and it was assumed as a continuous source for the entire time period of the solution.

Exponentially distributed point source concentration values were considered as the initial conditions of other spatial coordinates.

We begin the investigation by plotting the concentration breakthrough curves for the range of b , (0.0001 – 0.25 m), against a constant σ^2 of 0.001 for two different scales, 1 and 10 m flow lengths (Figure 1 and 2, respectively). Those two figures clearly show that stochasticity increases with the scale for similar parameters. At the 1 m flow length the stochastic behavior of almost all profiles are insignificant and at the 10 m flow is subject to high stochasticity.

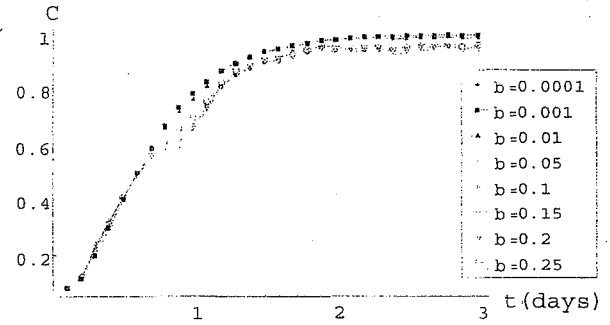


Figure 1. Concentration profile at $x = 0.5\text{m}$ of 1 m domain for $\sigma^2 = 0.001$.

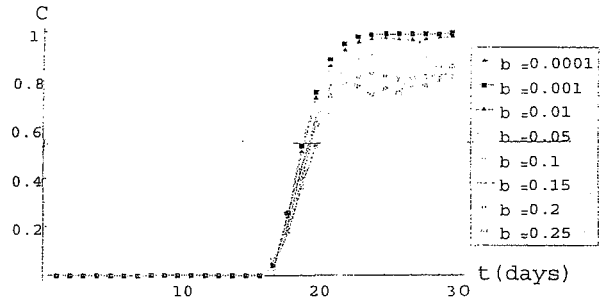


Figure 2. Concentration profiles at $x = 5\text{m}$ of 10 m domain for $\sigma^2 = 0.001$.

It may not be acceptable to depend on one set of Wiener process increments. Therefore, we tested the ability of SSTM to capture the scale dependency for different Wiener process increments as well. Figure 3 and Figure 4 demonstrate a sample of plots for 1 m and 10 m flow lengths, respectively. Those figures demonstrate that stochasticity has increased with the scale for similar parameters.

We continued the investigation of SSTM for other parameter combinations. Figure 5 and 7 show the concentration breakthrough curves for 1 m domain, and

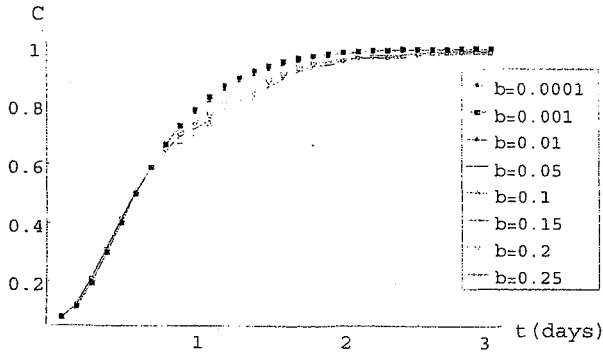


Figure 3. Concentration profiles at $x = 0.5\text{m}$ of 1 m domain for $\sigma^2 = 0.001$ with a different Wiener Process.

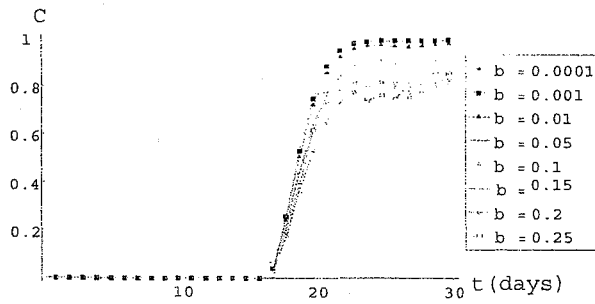


Figure 4. Concentration profiles at $x = 5\text{m}$ of 10 m domain for $\sigma^2 = 0.001$ with a different Wiener Process.

Figure 6 and 8 illustrate the concentration profiles for 10 m scale for comparable parameters, respectively. Those figures graphically verify that the potential of SSTM to capture the scale dependence. Figure 8 shows that even for larger scales the flow is reasonably stable for smaller σ^2 values, and as σ^2 increases the stochasticity of the flow intensifies.

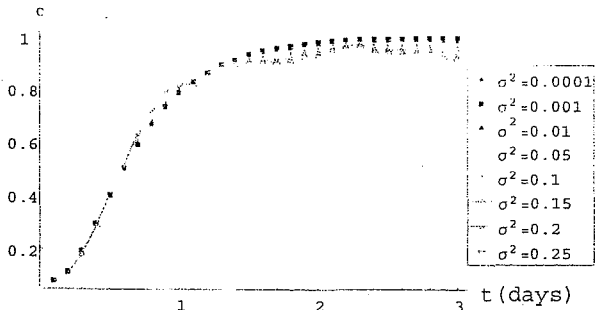


Figure 5. Concentration profiles at $x = 0.5\text{ m}$ of 1 m domain for $b = 0.001\text{ m}$.

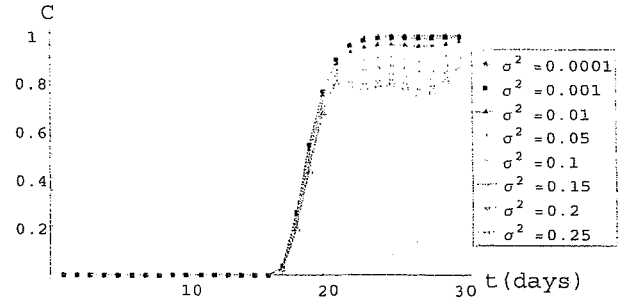


Figure 6. Concentration profiles at $x = 5\text{ m}$ of 10 m domain for $b = 0.001\text{ m}$.

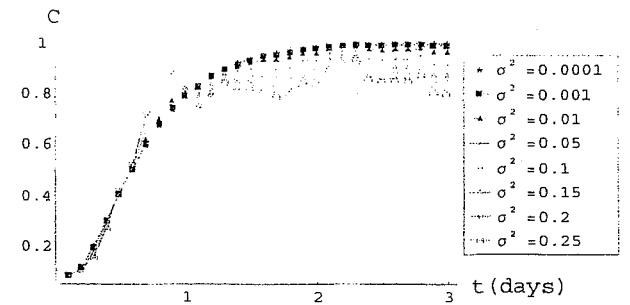


Figure 7. Concentration profiles at $x = 0.5\text{ m}$ of 1 m domain for $b = 0.01\text{ m}$.

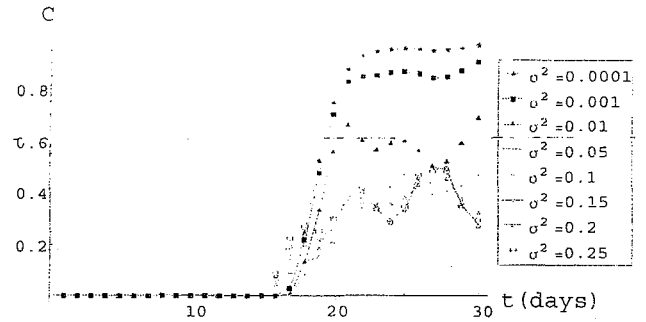


Figure 8. Concentration profiles at $x = 5\text{ m}$ of 10 m domain for $b = 0.01\text{ m}$.

We plotted the concentration breakthrough curves for range of b , ($0.0001 - 0.25\text{ m}$) against a constant σ^2 of 0.001 for a larger flow length of 20 m (Figure 9). Comparing Figure 1, 2 and 9 for similar parameter combinations for different scales, 1 , 10 and 20 m , exemplify that the rate of increase of stochasticity is decreasing with scale. Instability of the flow increases significantly from 1 m flow length to 10 m . However, further increase to 20 m does not illustrate considerable difference in increase of stochasticity.

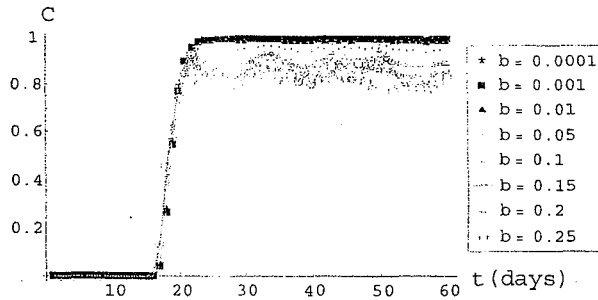


Figure 9. Concentration profiles at $x = 10$ m of 20 m domain for $\sigma^2 = 0.001$.

Even though similar model performances of scale dependence and decreasing rate of change of stochasticity are evident in other scales, visual comparison may not be sufficient to conclusively support the ability of capturing the scale dependency. Therefore, we explored the ways of estimating D of the flow to recognize the increase of stochasticity with scale.

Rajanayaka and Kulasiri [2002] showed that SSTM could mimic the advection-dispersion model with reasonable accuracy provided that an appropriate D was found. Hence, concentration profiles obtained from SSTM for spatial-temporal development were used to estimate the corresponding D of the advection-dispersion model. A stochastic inverse method (SIM) was employed to determine D [for details refer to Rajanayaka and Kulasiri, 2001]. In SIM we modeled the solute transport system through stochastic differential equations and obtained the likelihood expression for the estimation of parameters. Then, parameters were estimated using the maximum likelihood approach.

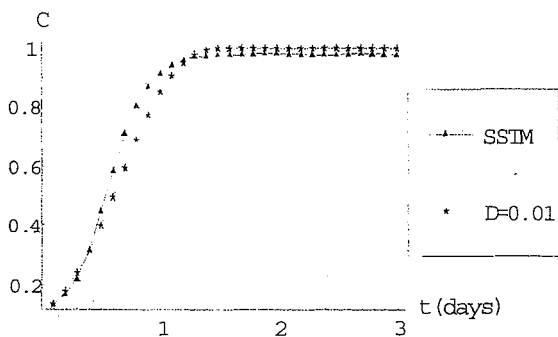


Figure 10. Comparison of deterministic advection-dispersion ($D = 0.01$) and stochastic ($\sigma^2 = 0.001$ and $b = 0.0001$) model concentration profiles.

Figure 10 demonstrates that the comparison of deterministic and stochastic concentration profiles for 1 m domain, where parameters of SSTM are $\sigma^2 = 0.001$ and $b = 0.0001$, and corresponding $D = 0.01$ m²/day for the advection-dispersion model. For the 10 m scale, Figure 11 shows that for the similar parameter values of SSTM, D has increased to 0.035 m²/day, i.e., the dispersivity of the flow of SSTM has increased with the scale for similar parameters.

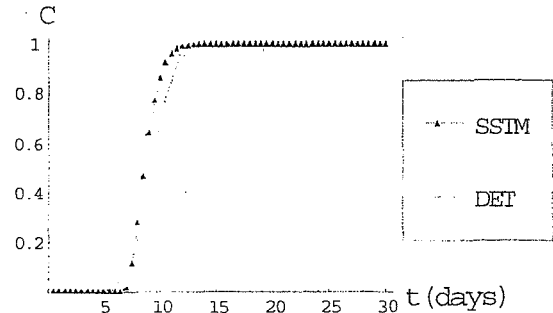


Figure 11. Comparison of deterministic advection-dispersion ($D = 0.035$) and stochastic ($\sigma^2 = 0.001$ and $b = 0.0001$) model concentration profiles for 10 m domain.

We further employed SIM to estimate D for other combinations of σ^2 and b for different flow lengths. Table 1 exhibits the estimated D for the range of scales; 1, 10, 20, 50 and 100 m.

Table 1, Figures 12 and 13 show that the values of estimated D increase with scale for same parameter combinations. Similarly, the estimates illustrate higher randomness for larger values of parameters for the same flow scale.

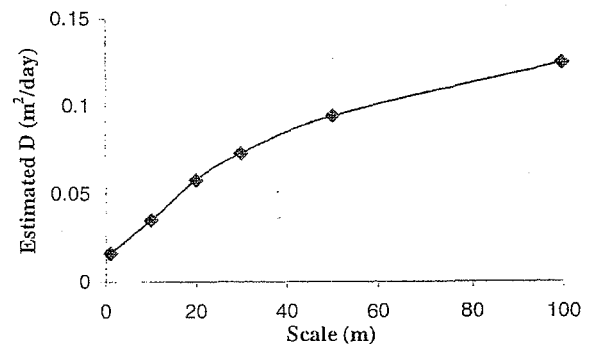


Figure 12. Scale dependence of D for parameter combination of $b = 0.0001$ and $\sigma^2 = 0.0001$.

Table 1. Estimates of D obtained by using a stochastic inverse method for different combinations of parameters of SSTM for different flow lengths (flow velocity = 0.5 m/day).

b	σ^2	Estimated D (m ² /day)					b	σ^2	Estimated D (m ² /day)				
		1 m	10 m	20 m	50 m	100 m			1 m	10 m	20 m	50 m	100 m
0.0001	0.0001	0.0163	0.0350	0.0580	0.0945	0.1249	0.1	0.1	0.0723	0.2970	0.4859	0.9336	1.4511
0.0001	0.001	0.0194	0.0374	0.0613	0.0993	0.1301	0.1	0.15	0.0749	0.2978	0.4766	0.9194	1.4211
0.0001	0.01	0.0384	0.0529	0.0847	0.1359	0.1829	0.1	0.2	0.0759	0.2988	0.4811	0.9338	1.4481
0.0001	0.05	0.0476	0.0780	0.1299	0.2065	0.2701	0.1	0.25	0.0761	0.2993	0.4854	0.9329	1.4503
0.0001	0.1	0.0679	0.0869	0.1421	0.2334	0.3121	0.1	0.3	0.0768	0.2979	0.4807	0.9136	1.4187
0.0001	0.15	0.0697	0.0906	0.1504	0.2402	0.3133	0.15	0.0001	0.0173	0.0878	0.1415	0.2868	0.4530
0.0001	0.2	0.0705	0.0926	0.1572	0.2576	0.3394	0.15	0.001	0.0257	0.1092	0.1805	0.3591	0.5634
0.0001	0.25	0.0719	0.0938	0.1591	0.2554	0.3329	0.15	0.01	0.0545	0.1622	0.2612	0.5280	0.8293
0.0001	0.3	0.0726	0.0947	0.1613	0.2603	0.3474	0.15	0.05	0.0657	0.2450	0.4046	0.8163	1.2785
0.001	0.0001	0.0192	0.0374	0.0552	0.0963	0.1298	0.15	0.1	0.0763	0.2483	0.4053	0.8210	1.2859
0.001	0.001	0.0375	0.0529	0.0802	0.1334	0.1827	0.15	0.15	0.0772	0.2490	0.4033	0.8209	1.2914
0.001	0.01	0.0674	0.0870	0.1353	0.2301	0.3177	0.15	0.2	0.0779	0.2502	0.4044	0.8103	1.2749
0.001	0.05	0.0742	0.0965	0.1531	0.2624	0.3639	0.15	0.25	0.0781	0.2528	0.4159	0.8368	1.3211
0.001	0.1	0.0849	0.0991	0.1552	0.2543	0.3522	0.15	0.3	0.0786	0.2567	0.4121	0.8321	1.3006
0.001	0.15	0.0867	0.1078	0.1744	0.2958	0.4075	0.2	0.0001	0.0172	0.0893	0.1477	0.3075	0.4862
0.001	0.2	0.0948	0.1189	0.1886	0.3256	0.4444	0.2	0.001	0.0243	0.1146	0.1875	0.3890	0.6197
0.001	0.25	0.1070	0.1293	0.2006	0.3382	0.4627	0.2	0.01	0.0516	0.1450	0.2309	0.4828	0.7726
0.001	0.3	0.1101	0.1386	0.2190	0.3683	0.5083	0.2	0.05	0.0658	0.2059	0.3329	0.6945	1.1091
0.01	0.0001	0.0254	0.0530	0.0804	0.1438	0.2066	0.2	0.1	0.0740	0.2301	0.3669	0.7767	1.2365
0.01	0.001	0.0570	0.0877	0.1344	0.2457	0.3475	0.2	0.15	0.0748	0.2451	0.3975	0.8412	1.3360
0.01	0.01	0.0791	0.1000	0.1533	0.2859	0.4047	0.2	0.2	0.0749	0.2570	0.4131	0.8656	1.3796
0.01	0.05	0.0946	0.1695	0.2673	0.4873	0.6933	0.2	0.25	0.0752	0.2665	0.4384	0.9342	1.4855
0.01	0.1	0.1148	0.2133	0.3345	0.6167	0.8792	0.2	0.3	0.0753	0.2739	0.4458	0.9324	1.4756
0.01	0.15	0.1375	0.2407	0.3717	0.6779	0.9666	0.25	0.0001	0.0169	0.0864	0.1404	0.2977	0.4755
0.01	0.2	0.1557	0.2599	0.4048	0.7380	1.0510	0.25	0.001	0.0229	0.1178	0.1935	0.4130	0.6598
0.01	0.25	0.1847	0.2712	0.4175	0.7508	1.0649	0.25	0.01	0.0483	0.1343	0.2209	0.4679	0.7493
0.01	0.3	0.1899	0.2775	0.4301	0.7859	1.1159	0.25	0.05	0.0619	0.1883	0.3066	0.6719	1.0812
0.05	0.0001	0.0187	0.0783	0.1247	0.2300	0.3421	0.25	0.1	0.0747	0.2323	0.3771	0.8150	1.3063
0.05	0.001	0.0356	0.1013	0.1625	0.2995	0.4468	0.25	0.15	0.0754	0.2502	0.4122	0.8866	1.4280
0.05	0.01	0.0696	0.1599	0.2521	0.4535	0.6801	0.25	0.2	0.0756	0.2658	0.4288	0.9262	1.4867
0.05	0.05	0.0765	0.2627	0.4132	0.7556	1.1305	0.25	0.25	0.0757	0.2810	0.4607	0.9976	1.6044
0.05	0.1	0.0845	0.2921	0.4587	0.8399	1.2649	0.25	0.3	0.0759	0.2916	0.4695	1.0001	1.6102
0.05	0.15	0.0873	0.2966	0.4746	0.8836	1.3314	0.3	0.0001	0.0179	0.0823	0.1391	0.3154	0.5140
0.05	0.2	0.0899	0.2970	0.4684	0.8521	1.2774	0.3	0.001	0.0217	0.1102	0.1854	0.4242	0.6926
0.05	0.25	0.0922	0.2948	0.4669	0.8705	1.3099	0.3	0.01	0.0479	0.1486	0.2529	0.5811	0.9525
0.05	0.3	0.0929	0.2914	0.4575	0.8394	1.2643	0.3	0.05	0.0632	0.2214	0.3815	0.8727	1.4254
0.1	0.0001	0.0180	0.0855	0.1424	0.2690	0.4210	0.3	0.1	0.0753	0.2517	0.4278	0.9778	1.5873
0.1	0.001	0.0297	0.1054	0.1686	0.3162	0.4856	0.3	0.2	0.0780	0.2876	0.4900	1.1133	1.8145
0.1	0.01	0.0593	0.1780	0.2910	0.5682	0.8849	0.3	0.25	0.0782	0.2980	0.5067	1.1705	1.9103
0.1	0.05	0.0645	0.2818	0.4533	0.8774	1.3585	0.3	0.3	0.0791	0.3070	0.5375	1.2230	1.9850

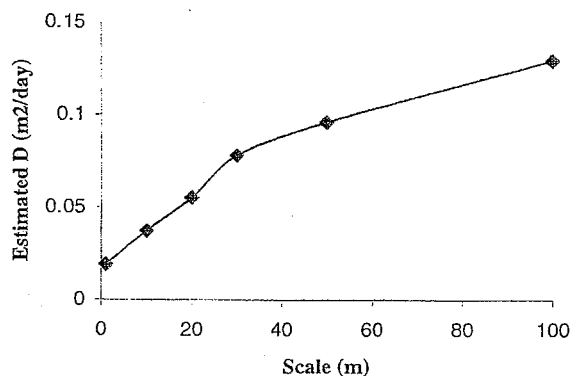


Figure 13. Scale dependence of D for parameter combination of $b = 0.001$ and $\sigma^2 = 0.0001$.

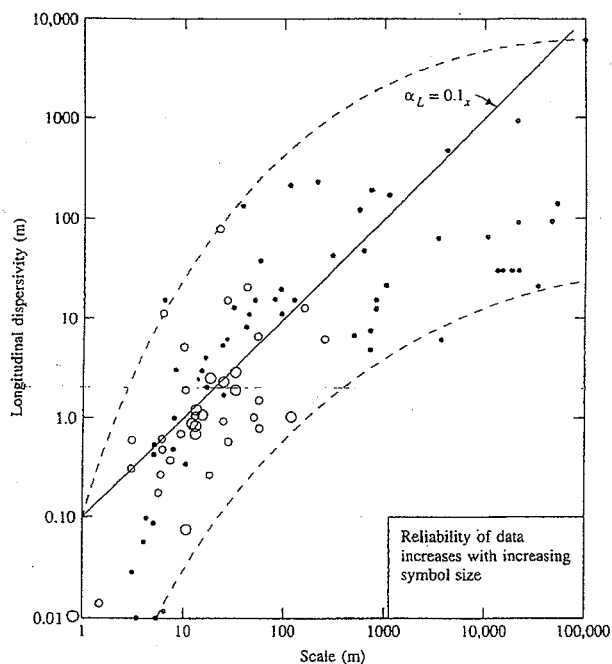


Figure 14. Field measured values of α_L as a function of the scale of measurement. The largest circles represent the most reliable data. Source: Gelhar [1986].

Pickens and Grisak [1981], and Lallemand-Barres and Peaudecerf [1978] showed that the scale dependency of α_L has a linear relationship of $\alpha_L = 0.1 L$, where L is the mean travel distance. However, Pickens and Grisak [1981] recognized that the linear increase of dispersivity with the mean travel distance was unlikely for large travel distances.

It was expected that tracer migration between aquifer layers could cause a reduction in the magnitude of the proportionality constants, since transverse migration would tend to reduce the spreading effect caused by the stratification. The field measurements obtained by Gelhar [1986] illustrates that the scale dependence relationship between α_L and the flow length is non-linear (Figure 14).

To evaluate the comparative estimates of D obtained from the inverse method for SSTM parameters and the field measurements observed by Gelhar [1986], we plotted them in a same plot (Figure 15). Only reliable observations of Figure 14 (indicated by larger symbols) were considered. Since, the parameter estimated from the inverse approach was D , α_L values of Figure 14 were converted to D ($D = \alpha_L v$). Further, we plotted the relationship of $\alpha_L = 0.1 L$ in the same graph to assess our estimates. A mid range of b , 0.01 m, from Table 1 was chosen for the plot as to consider average parameter value of SSTM.

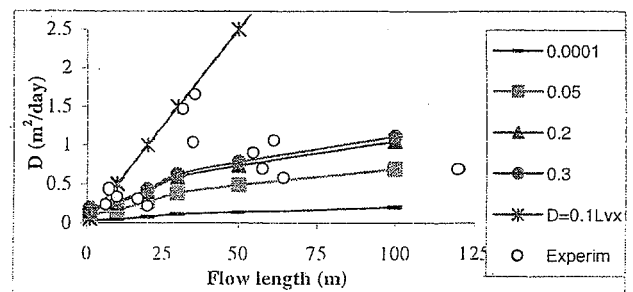


Figure 15. Estimated D values for $b = 0.01$ for range of σ^2 (0.0001 – 0.3), $D = 0.1 L v$, and reliable field measurements observed by Gelhar [1986] for different flow lengths.

Figure 15 demonstrate that corresponding D values obtained for SSTM parameters do not agree with the relationship of $\alpha_L = 0.1 L$. However, they are in reasonable agreement with most of the reliable field measurements observed by Gelhar [1986].

4. CONCLUSION

In this paper we investigated the ability of a stochastic solute transport model (SSTM) to capture the scale dependency of solute dispersion in porous media. SSTM is capable of capturing the scale dependency of α_L that increases with the flow lengths in a non-linear fashion. The corresponding D values estimated for SSTM parameters give similar pattern of behavior with some experimental data in past literature. The main advantage of SSTM is that

can be utilized to describe different flow lengths without changing the parameters. Similar parameters of SSTM manifest smaller dispersivity for the smaller flow lengths and it progressively increases with the scale to reach an asymptotic value. Hence, SSTM can be used to model the dispersion at different flow lengths ranging from local to global scales.

Acknowledgment- Authors are grateful to Rania Sahioun, Lincoln University, New Zealand for her assistance in conducting computational experiments for this study.

5. REFERENCE

- Fetter, C.W. *Contaminant hydrogeology*. New Jersey: Prentice-Hall, 1999.
- Fried, J. J. Miscible pollution of ground water: A study of methodology. In A. K Biswas (Eds.). *Proceedings of the International Symposium on Modeling techniques in Water Resources Systems*, vol 2, 362-371. Ottawa, Canada, 1972.
- Fried, J.J. *Groundwater pollution*. Amsterdam: Elsevier Scientific Publishing Company, 1975.
- Gelhar, L.W. Stochastic subsurface hydrology from theory to applications. *Water Resources Research*, 22, (9), 135S-145S, 1986.
- Huang, K., Van Genuchten, M.T., & Zhang, R. Exact solution for one-dimensional transport with asymptotic scale dependent dispersion. *Applied Mathematical Modelling*, 20 (4), 298-308, 1996a.
- Huang, K., Toride, N., & Van Genuchten, M.T. Experimental investigation of solute transport in large, homogeneous heterogeneous, saturated soil columns. *International Journal of Rock Mechanics and Mining Sciences*, 33 (6), 249A, 1996b.
- Klenk, I.D., & Grathwohl, P. Transverse vertical dispersion in groundwater and the capillary fringe. *Journal of Contaminant Hydrology*, 58 (1-2), 111-128, 2002.
- Klotz, D., Seiler, K.-P., Moser, H., & Neumaier, F. Dispersivity and velocity relationship from laboratory and field experiments. *Journal of Hydrology*, 45 (1/2), 169-184, 1980.
- Kulasiri, D., & Verwoerd, W.S. A stochastic model for solute transport in porous media: mathematical basis and computational solution. In *Proceedings of the MODSIM 1999 International congress on modelling and simulation*. Hamilton: New Zealand; 31-36, 1999.
- Kulasiri, D., & Verwoerd, W. *Stochastic Dynamics: Modeling Solute Transport in Porous Media*, North-Holland Series in Applied Mathematics and Mechanics, vol 44. Amsterdam: Elsevier Science Publishes, 2002.
- Lallemant-Barres, P. & Peaudecerf, P. Recherche des relations entre la valeur de la dispersivite macroscopique d'un milieu aquifere, ses autres caracteristiques et les conditions de mesure, etude bibliographique. *Bulletin, Bureau de Recherches Geologiques et Minieres. Sec. 3/4*, 277-287, 1978.
- Oakes, D. B. & Edworthy, D. J. Field measurements of dispersion coefficients in the United Kingdom. In *groundwater quality, measurement, prediction and protection*, Water Research Centre, England, 327-340, 1977.
- Øksendal, B. *Stochastic Differential Equations*. Berlin: Springer Verlag, 1998.
- Pickens, J.F., & Grisak, G.E. Scale-dependent dispersion in a stratified granular aquifer. *Water Resources Research*, 17 (4), 1191-1211, 1981.
- Rajanayaka, C., & Kulasiri, D. Investigation of a parameter estimation method for contaminant transport in aquifers. *Journal of Hydroinformatics*, 3(4): 203-213, 2001.
- Rajanayaka, C., & Kulasiri, D. Exploration of the behaviour of a stochastic solute transport model using computational experiments. In *Proceeding of Biennial Congress of the International Environmental Modelling and Software Society (IEMSS) 2002*, Lugano, Switzerland: vol 2, 301- 306, 2002.
- Scheibe, T., & Yabusaki, S. Scaling of flow and transport behavior in heterogeneous groundwater systems, *Advances in Water Resources*, 22 (3), 223-238, 1998.
- Theis, C. V. Notes on dispersion I fluid flow by geologic features. In J. M Morgan, D. K Kamison and J. D. Stevenson (Eds.). *Proceedings of Conference on Ground Disposal of Radioactive Wastes*. Chalk River, Ont., Canada, 1962.
- Theis, C. V. Hydrologic phenomena affecting the use of tracers in timing ground water flow. *Radioisotopes in Hydrology*, 193-206, 1963.
- Vanderborght, J., & Vereecken, H. Estimation of local scale dispersion from local breakthrough curves during a tracer test in a heterogeneous aquifer: the Lagrangian approach. *Journal of Contaminant Hydrology*, 54 (1-2), 141-171, 2002.